

ROLE OF ULTRASOUND IN MORPHOLOGIC AND FUNCTIONAL ASSESSMENT OF FETAL HEART IN DIABETIC MOTHERS

Thesis

In partial fulfillment of Master Degree In radiology

Submitted By

Sameh Abdel Latif Abdel Salam

(M.B.B.Ch.), Cairo University

Supervised by

Prof. Soha Talaat Hamed

Prof. of Radiology

Faculty of Medicine, Cairo University

Prof. Mohamed Ali Abdel Kader

Prof. of Obstetrics and Gynecology

Faculty of Medicine, Cairo University

Dr. Mariam Raafat Lewis

Lecturer of Radiology

Faculty of Medicine, Cairo University

Faculty of Medicine

Cairo University

2015

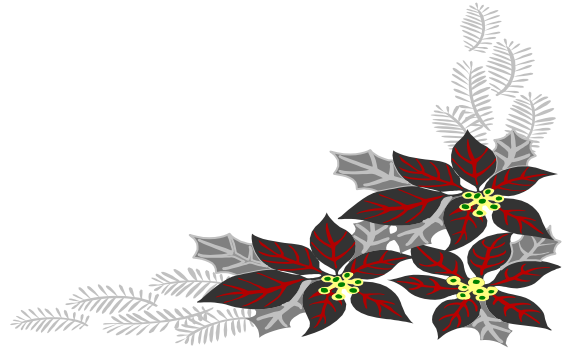


بِسْمِ اللَّهِ الرَّحْمَنِ الرَّحِيمِ

[قَالُوا سُبْحَانَكَ لَا عِلْمَ لَنَا إِلَّا مَا عَلَّمْتَنَا
إِنَّكَ أَنْتَ الْعَلِيمُ الْحَكِيمُ]

صدق الله العظيم

سورة البقرة الآية ٣٣





Acknowledgements

*At first and foremost, I thank the great **God** who gave me the power to finish this work,*

*No words can express my gratitude to **Prof. Dr. Soha Talaat Hamed**, Professor of radiology, Faculty of Medicine, Cairo University for her unlimited support and maternal advice. I was honored to work under her supervision.*

*I want to express my deepest gratitude to **Prof. Dr. Mohammed Ali Abdel Kader**, Professor of Obstetrics and Gynecology, Faculty of Medicine, Cairo University for his sincere supervision and advice. I was privileged to work under his generous supervision.*

*To **Dr. Mariam Raafat Lewis**, lecturer of radiology, Faculty of Medicine, Cairo University I owe a lot of thanks and gratitude for her support, patience and supervision.*

*To **my parents**, no words can express my gratitude for you; you are really the gifts of the great God.*

To my family, colleagues and everyone participated in this work by a way or another I owe my appreciation.

Abstract

Objective: To review the impact of maternal pre gestational and gestational diabetes on fetal cardiac morphology and function through assessment of cardiac structure, ventricular myocardial and septal hypertrophy and overall systolic and diastolic cardiac function using left modified myocardial performance index. **Design:** Case control study. **Subjects:** Twenty diabetic mothers and 30 control ones between 28 and 40 weeks gestational age. **Methods:** Fetal echocardiogram was done for diabetic patients, basic and extended basic cardiac exam for control cases. 2D measurement of end diastolic thickness of inter ventricular septum and ventricular myocardial free walls for all subjects with assessment of cardiac function using left modified myocardial performance index. **Results:** Statistically significant difference was detected between diabetic and control cases regarding septal and myocardial thickness denoting onset of fetal diabetic hypertrophic cardiomyopathy. Statistically significant left myocardial performance index between the 2 groups was found denoting impaired fetal cardiac overall systolic and diastolic function. One of the diabetic mothers was diagnosed with visceral heterotaxy syndrome (left isomerism). **Conclusion:** Maternal diabetes is strongly associated with fetal cardiac structural defects and should be considered as a high risk factor for congenital heart disease. Fetal cardiac hypertrophic cardiomyopathy with impairment of cardiac function occurs with maternal diabetes. Further research should focus on strict metabolic control of maternal diabetes as it may help in prevention of this functional impairment with postnatal follow up for evaluation of regression of cardiac condition on regular medical treatment.

Keywords:

Fetal echocardiography, Maternal diabetes, Hypertrophic cardiomyopathy,
Myocardial performance index.

List of Contents

Title	Page
List of Abbreviations	I
List of Tables	IV
List of Figures	V
Introduction	1
Aim of the Work	2
Review of Literature	
Chapter I: Ultrasound Physics and Instrumentation	3
Chapter II: Normal Ultrasonic Anatomy of the Fetal Heart	22
Chapter III: Technical aspects in fetal echocardiography	41
Chapter IV: Functional assessment of the fetal heart	54
Chapter V: Sonographic features of abnormal fetal heart	70
Chapter VI: Fetal cardiac effects of maternal hyperglycemia during pregnancy	111
Patients and Methods	117
Results	120
Case presentation	131
Discussion	143
Summary	154
Conclusion and Recommendations	156
References	157
Arabic Summary	

List of Abbreviations

2D	To-dimensional
3D	Three-dimensional
4D	Four-dimensional
ADF	Advanced dynamic flow
AIUM	American institute of ultrasound in medicine
Ao	Aorta
APVS	Absent pulmonary valve syndrome
ARSA	Aberrant right subclavian artery
AS	Aortic stenosis
ASA	Atrial septal aneurysm
ASD	Atrial septal defect
AV	Atrioventricular
AVB	Atrioventricular block
AVNRT	Atrioventricular nodal reentrant tachycardia
AVRT	Atrioventricular reentrant tachycardia
AVSD	Atrioventricular septal defect
ccTGA	Congenitally corrected transposition of the great arteries
CDF	Color Doppler flow
CHD	Congenital heart disease
CHF	Congestive heart failure
CM	Cardiomyopathy
DORV	Double-outlet right ventricle
EDF	End-diastolic flow
EFE	Endocardial fibroelastosis
Hb.	Hemoglobin
HIFU	High-intensity focused ultrasound
HLHS	Hypoplastic left heart syndrome
HRHS	Hypoplastic right heart syndrome
Hz	Hertz
IAA	Interrupted aortic arch
IPT	Intraperitoneal transfusion
ICT	Isovolumic contraction time
IRT	Isovolumic relaxation time
ISUOG	International Society of Ultrasound in Obstetrics and gynecology
IVC	Inferior vena cava
IVS	Intact ventricular septum
IVT	Intravascular transfusion
KHz	Kilohertz
LAI	Left atrial isomerism

LSVC	Left superior vena cava
LVNC	Left ventricular non-compaction cardiomyopathy
LVOT	Left ventricular outflow tract
MHz	Megahertz
MI	Mechanical index
MPI	Myocardial performance index
RVWT	Right ventricular wall thickness
MPa	Megapascal
MR	Mitral regurgitation
NC	Non-compaction
PA	Pulmonary artery
PA: IVS	Pulmonary atresia with intact ventricular septum
PDU	Power Doppler ultrasound
PI	Pulsatility index
PJRT	Permanent junctional reciprocating tachycardia
PR	Pulmonary regurgitation
PS	Pulmonary stenosis
PSV	Peak systolic velocity
PSVT	Paroxysmal supraventricular tachycardia
PZT	Lead zirconate titanate
RAA	Right aortic arch
RAI	Right atrial isomerism
RI	Resistance index
ROI	Region of interest
RVOT	Right ventricular outflow tract
SD	Standard deviation
SIV	Situs inversus
SonoAVC	Sonographic automated volume calculation
STIC	Spatio-temporal image correlation
SV	Single ventricle
SVC	Superior vena cava
SVT	Supraventricular tachycardia
TA	Tricuspid atresia
TAPVC	Total anomalous pulmonary venous connection
TCI	Tissue compound imaging
TDI	Tissue Doppler imaging
Tei	Myocardial performance index
TF4	Tetralogy of Fallot
TGA	Transposition of the great arteries
TI	Thermal index
TIB	Thermal index for bone
TIC	thermal index for cranial bone

TIS	Thermal index for soft tissue
TR	Tricuspid regurgitation
TUI	Tomographic ultrasound imaging
US	Ultrasound
VCAD	Volume computer aided diagnosis
VCI	Volume contrast imaging
VOCAL	Volume computer aided analysis
VOI	Volume of interest
VSD	Ventricular septal defect
LVWT	Left ventricular wall thickness
IVST	Interventricular septal thickness

List of Tables

Tables	
1	Paired T test for Comparison between IVST Patients and controls
2	Paired T test for Comparison between RVWT Patients and controls
3	Paired T test for Comparison between LVWT Patients and controls
4	T test for Comparison between Tei index for Patients and controls

List of Figures

Figures	
1	Ultrasound Transducer
2	Axial and lateral resolution (www.alnmag.com)
3	Wavelength, amplitude and frequency (www.encyclopedia.com)
4	Reflection, refraction and attenuation
5	Right image: frequency compound imaging at 10 MHz; left image: Tissue harmonic imaging (breast speculated mass better)
6	Volume contrast imaging (VCI) in the C-plane: In the axial scan a line is selected passing through the cavum septi pellucidi between the two hemispheres. The sagittal view (C-plane) orthogonal the axial one is simultaneously displaced showing the corpus callosum
7	The Doppler equation (www.centrus.com)
8	Resistance indices for Doppler waveform analysis (www.fetalmedicinefoundation.org)
9	Drawing of cardiac tube www.Medical embryology.org 2006
10	Formation of the atrial septum. www.medicalembryology.org)
11	Formation of ventricular septum
12	Degenerated aortic arch arteries and the final great vessels anatomy
13	(labeled 4 chamber anatomy, RV: right ventricle, LV: left ventricle, RA: right atrium, LA: left atrium, FO: foramen ovale, Chaoi et al., 1994)
14	(Schematic drawings of fetal cardiac sections, Yoo et al., 1997)
15	Normal four-chamber view
16	Septum primum and foramen ovale
17	(Fetal abdominal situs, Abohamad, 1997)
18	Fetal cardiac axis (Allan, 2000). The dashed line refers to the line bisecting the chest from anterior to posterior passing through the spine. The continuous line refers to the long axis of the fetal heart forming an angle with the dashed line equals 45 ± 20 .
19	Color Doppler at the level of 4 chamber view showing pulmonary veins entering the left atrium

20	Color Doppler of the four-chamber view (www.Woemensimag-ingservices.com)
21	Left ventricular outflow tract
22	Basal short axis view showing right ventricular outflow tract (www.iame.com)
23	Three-vessel view
24	Longitudinal view of the aortic arch showing neck vessels (arrowheads)
25	Sagittal view of ductal arch
26	Caval long-axis view (www. The fetus.net)
27	(tomographic ultrasound cuts of fetal cardiac sections to illustrate anatomy from situs to 3 vessel view, Devore et al., 2003)
28	Multiplanar reconstruction with rendered
29	Four-chamber view: Surface volume rendering
30	Spin technique
31	Tomographic Ultrasound Imaging
32	Inversion mode: Fetal heart
33	Inversion mode in a fetus with TGA
34	B-flow: aortic overriding and discrepancy in size of aorta and pulmonary arteries in the context of tetralogy of Fallot
35	VOCAL: Fetal heart volume assessment
36	Sono AVC: Measurement of the fetal right ventricular volume
37	Sono AVC: Hypoplastic left heart syndrome
38	3D color Doppler: 3D volume rendering with transparent gray-scale and surface color Doppler of a fetus with TGA
39	3D color Doppler measurement of cardiac output
40	Advanced Dynamic Flow: Aortic overriding
41	Graph representing phases of cardiac cycle From Wikimedia Commons.com
42	(Graphic representation of the three-directional myocardial motility involving longitudinal, radial and circumferential contraction. The motion is shown as a single point motility determined by displacement and systolic (S') and early diastolic (E') annular peak velocities; and deformation by the change in length or thickness between two points represented as strain or strain rate
43	Graph showing parallel fetal circulation (www. American heart association.org)

44	Right and left ventricular outflow tracts for measuring stroke volume (SV) and cardiac output (CO). The valve diameter (D) is measured in a 2D image. Velocity time integral (VTI) of the blood flow and heart rate (HR) are evaluated in the spectral Doppler waveform. Combined cardiac output (CCO) is calculated by the sum of both CO, and cardiac index (CI) represents the normalization by estimated fetal weight (EFW) (Gratacós et al., 2013)
45	Mitral E/A waveform (Andrade et al., 2012)
46	Mechanical PR interval, DeVore, 2005). E: early diastolic filling, A: late diastolic filling = atrial contraction, 1=start of A wave, 2=start of V wave, PR interval:from 1 to 2.
47	(Illustration of myocardial performance index (MPI) assessment by spectral Doppler) (Gratacós et al., 2013). ICT: Isovolumetric contraction time, ET: Ejection time, IRT: Isovolumetric relaxation time.
48	Illustration of a transverse four-chamber view in order to measure shortening (SF) and ejection fractions (EF) of the right (RV) and left ventricles (LV) by M-mode
49	(M mode tracing of tricuspid annular plane systolic excursion)
50	early (E') and late (A') diastolic and systolic (S') peak annular velocities obtained by spectral tissue Doppler at the right annulus
51	Offline analysis of strain (above) and strain rate (below) waveforms at the right basal free wall using color tissue Doppler
52	Post-processing analysis of the left ventricular volume through virtual organ computerized analysis using 4D-spatio temporal correlation
53	Atrial septal defect in the context of atrio ventricular canal defect
54	VSD depiction by power Doppler
55	Normal atrioventricular valves
56	Atrioventricular septal defect
57	2D image of 4 chamber view showing atrial septal aneurysm
58	Ebstein's anomaly
59	Tricuspid valve atresia
60	Stenotic tricuspid valve
61	Hypoplastic right heart

62	Hypoplastic left heart syndrome
63	Absent pulmonary valve syndrome (www.the fetus.net)
64	Pulmonary atresia with intact ventricular septum
65	Right atrial isomerism: The ultrasonic picture shows the juxtaposition of the descending aorta and the inferior vena cava
66	Left isomerism: Interrupted inferior vena cava with azygos continuation
67	Ectopia cordis with normal heart anatomy
68	Tetralogy of Fallot: Perimembranous ventricular septal defect and overriding aorta
69	Double outlet right ventricle: Parallel course of great vessels (www.the fetus.net)
70	Transposition of the great arteries
71	Congenitally corrected TGA
72	Common arterial trunk
73	Aortic coarctation
74	Interrupted aortic arch. Sagittal view of the fetal thorax showing characteristic straight course of the aortic arch with typical V pattern of its branches diagnostic of type B IAA
75	Aberrant right subclavian artery. Axial view of fetal thorax showing confluence of ductal and aortic arches with aberrant course of right subclavian artery originating from isthmus portion of aortic arch and coursing retroesophageal from left to right side
76	Right aortic arch with tetralogy of Fallot
77	Complete vascular ring in the context of double aortic arch
78	Schematic drawing of TAPVC: A: TAPVC supracardiac form into left innominate vein, B: TAPVC supracardiac form into right SVC, C: TAPVC form into coronary sinus, TAPVC infracardiac infra diaphragmatic form into Hepatic vasculature (Hepatic veins or portal vein or may into IVC) (www.springerimages.com)
79	Interrupted IVC: The dilated azygos is seen with no evidence of IVC in the left image
80	Dilated cardiomyopathy
81	Non-compaction cardiomyopathy in short axis view
82	Rhabdomyoma. The right one is small and not obstructing inflow or outflow tracts of the left ventricle while the left one is huge obstructing left ventricular

	inflow and causing heart failure (pericardial effusion) and pulmonary hypoplasia (www.fetalsono.com).
83	Simultaneous Doppler placement on aorta and SVC
84	Atrial flutter: M-mode recording
85	Supraventricular tachycardia with short VA interval
86	Echogenic cardiac focus (www.the fetus.net)
87	Linear regression curve to illustrate significant correlation between IVST for both patients and controls (Correlation coefficient $R^2=0.244$)
88	Linear regression curve to illustrate significant correlation between RVWT for both patients and controls (Correlation coefficient $R^2=0.206$)
89	Linear regression curve to illustrate significant correlation between LVWT for both patients and controls (Correlation coefficient $R^2=0.32$)
90	Linear regression curve to illustrate significant correlation between Tie index for both patients and controls (Correlation coefficient $R^2=0.039$)
91	Normal values of tie index in 5 th , 50 th and 95 th percentile curves in our third trimester control cases plotted against gestational age (range from 0.32 to 0.62, median=0.47)
92	Normal values of IVST in 5 th , 50 th and 95 th percentile curves in our third trimester control cases plotted against gestational age (range from 0.35 to 0.67, median 0.45)
93	Normal values of LVWT in 5 th , 50 th and 95 th percentile curves in our third trimester control cases plotted against gestational age (range from 0.34 to 0.58, median = .42)
94	Normal values of RVWT in 5 th , 50 th and 95 th percentile curves in our third trimester control plotted against gestational age (range from 0.32 to 0.64, median=0.46)
95	5 th , 50 th , 95 th percentile curves for tie index measured in our diabetic patients plotted against gestational age (range from 0.39 to 0.83, median= 0.61)
96	5 th , 50 th , 95 th percentile curves for the IVST measured in our diabetic cases plotted against gestational age (range from 0.46 to 0.9, median 0.7)
97	5 th , 50 th , 95 th percentile curves for the RVWT measured in diabetic cases plotted against gestational age (range from 0.39 to 0.79, median = 0.0.73)

98	5 th , 50 th , 95 th percentile curves for the measured LVWT in diabetic cases plotted against gestational age (range from 0.38 to 0.93, median = 0.75))
99	2D measurement of myocardial and septal wall thickness in lateral 4 chamber view
100	Doppler derived measurement of left modified myocardia performance index (tie index=0.4)
101	2D measurement of myocardial and septal wall thickness in lateral 4 chamber view
102	Doppler derived measurement of left modified myocardial performance index (tie index=0.43)
103	2D measurement of myocardial and septal wall thickness in lateral 4 chamber view
104	Doppler derived measurement of left modified myocardial Performance index (tie index=0.69)
105	2D measurement of myocardial and septal wall thickness in lateral 4 chamber view
106	Doppler derived measurement of left modified myocardial performance index (tie index=0.85)
107	2D measurement of myocardial and septal wall thickness in lateral 4 chamber view
108	Doppler derived measurement of left modified myocardial performance index (tie index=0.5)
109	2D measurement of myocardial and septal wall thickness in lateral 4 chamber view
110	Doppler derived measurement of left modified myocardial performance index (tie index=0.61)
111	2D measurement of myocardial and septal wall thickness in apical 4 chamber view
112	Doppler derived measurement of left modified myocardial performance index (tie index=0.5)
113	(Hemiazygos vein behind the descending aorta in upper abdominal axial image. Ao: Aorta, HAZ: Hemi azygos vein).
114	Stomach is left but with more central inclination (gastric mal rotation) St: Stomach
115	4 chamber view showing mitral Artesia, hypoplastic left ventricle, dilated right ventricle and Hemi azygos vein. Ao: Aorta, HAZ: hemi azygos vein, LV: Left Ventricle. RV: right ventricle, RA: right atrium, TV: tricuspid valve.)